IVYSPRING INTERNATIONAL PUBLISHER

Theranostics

2016; 6(3): 418-427. doi: 10.7150/thno.14018

Research Paper

Gadolinium-Based Nanoparticles and Radiation Therapy for Multiple Brain Melanoma Metastases: Proof of Concept before Phase I Trial

Shady Kotb[1], Alexandre Detappe[1,2,3], François Lux[1], Florence Appaix[4], Emmanuel L. Barbier[4,5], Vu-Long Tran[1], Marie Plissonneau[1,3], Hélène Gehan[1,3], Florence Lefranc[6], Claire Rodriguez-Lafrasse[7], Camille Verry[8], Ross Berbeco[2], Olivier Tillement[1], Lucie Sancey[1]✉

1. Institut Lumière Matière, UMR5306, Université Claude Bernard Lyon1-CNRS, Université de Lyon 69622 Villeurbanne Cedex, France
2. Department of Radiation Oncology, Brigham and Women's Hospital, Dana-Farber Cancer Institute and Harvard Medical School, Boston, MA, United States
3. Nano-H, St Quentin Fallavier, 38070, France
4. Grenoble Institut des Neurosciences (GIN), INSERM U836, Grenoble, 38706, France
5. Université Grenoble Alpes, Grenoble, France
6. Service de Neurochirurgie, Hôpital Erasme, Université Libre de Bruxelles, 808 Route de Lennik, 1070 Brussels, Belgium
7. Laboratoire de Radiobiologie Cellulaire et Moléculaire, EMR3738, Faculté de Médecine Lyon-Sud, Université de Lyon, Université Lyon 1, Oullins, France
8. Radiotherapy Department, Grenoble University Hospital, 38043 Grenoble.

✉ Corresponding author: Lucie Sancey PhD. Institut Lumière Matière, Equipe FENNEC - UMR CNRS 5306 - Univ. Lyon 1, Bâtiment Jules Raulin, 2, rue V. Grignard, 69622 Villeurbanne Cedex FRANCE. E-mail: lucie.sancey@univ-lyon1.fr. Phone: +33 4.27.46.57.24

Received: 2015.10.01; Accepted: 2015.12.12; Published: 2016.01.20

Abstract

Nanoparticles containing high-Z elements are known to boost the efficacy of radiation therapy. Gadolinium (Gd) is particularly attractive because this element is also a positive contrast agent for MRI, which allows for the simultaneous use of imaging to guide the irradiation and to delineate the tumor. In this study, we used the Gd-based nanoparticles, AGuIX®. After intravenous injection into animals bearing B16F10 tumors, some nanoparticles remained inside the tumor cells for more than 24 hours, indicating that a single administration of nanoparticles might be sufficient for several irradiations. Combining AGuIX® with radiation therapy increases tumor cell death, and improves the life spans of animals bearing multiple brain melanoma metastases. These results provide pre-clinical proof-of-concept for a phase I clinical trial.

Key words: AGuIX, radiosensitizer, radiation therapy, brain metastases, nanoparticles, imaged-guided therapy, personalized medicine

Introduction

Despite recent outcome progress,[1-3] melanoma is still difficult to treat due to multidrug- and radio-resistance and high metastatic capacity.[4] In approximately 80% of cases, malignant melanomas tend to metastasize into the central nervous system;[5] this specific dissemination has a considerable effect on overall patient survival. Neurosurgeons and neuro-oncologists have attained limited success using conventional treatments such as surgical resection[6, 7] when possible, and radiation therapy with local approach,[8] stereotactic radiosurgery,[9] or *in toto* radiation with whole-brain radiotherapy (WBRT).[10]

One method for enhancing the effect of radiotherapy is to combine X-ray radiation exposure with metallic nanoparticles containing high-Z atoms. This approach has been known for at least 10 years,[11] and is based on the interaction of low-energy photons with these elements.[12-14] During this interaction, photons are absorbed by the nanoparticles, which subsequently release photoelectrons and Auger electrons, leading to a local dose enhancement and the creation of reactive oxygen species (ROS), damaging the neighboring cells.[15] After IV injection, the particles can reach the tumor site through the passive en-

hanced permeability and retention effect (EPR effect).[16, 17] Gd-based nanoparticles are not only a radiosensitizer under the presence of photons at different energies, ions (such as He^{2+}, 150 MeV/µma, linear energy transfer (LET) 2.33 KeV/µm) and hadrons (C^{6+}, 200 MeV/µma, LET 13 KeV/µm),[17-20] they can also act as T1 contrast agents for MRI.[13, 17, 21-23] Therefore, they act as dual modality agents with both diagnostic and therapeutic applications.

This paper focuses on radiotherapy enhancement using small Gd-based nanoparticles, named AGuIX® (Activation and Guidance of Irradiation by X-ray). The study includes both a cellular model and a pre-clinical model consisting of multiple brain melanoma metastases to provide a proof of concept for a short term clinical trial for this pathology. *In vitro,* the combination of the nanoparticles and 2 Gy radiation was 52 % higher compared with radiation alone, with a significant increase in double strand breaks (DSBs), although the particles remained outside the nucleus. *In vivo* MRI confirmed the uptake of the nanoparticles by B16F10 brain metastases and increased during more than 3.5 hours as confirmed by two-photon confocal imaging. In addition, the signal remained for 24 hours after injection. This long period of uptake allows the treatment to be performed for at least 2 continuous days. The 7-Gy dose delivery increased the life spans of mice bearing multiple brain melanoma metastases by 8.3 %, whereas the combined treatment allowed an increase of up to 25 % compared with untreated mice, *i.e.*, a threefold higher treatment efficacy.

Materials and methods

Cell culture

B16F10 cells (# CRL-6475, LGC Promochem, Molsheim France), which are mouse skin melanoma cells, were cultured in Dulbecco's Modified Eagle Medium supplemented with 10 % fetal bovine serum (Pan-Biotech) and 1 % penicillin-streptomycin glutamine (Pan-Biotic).[24] Cells were grown in a humidified incubator at 37°C and 5 % CO_2.

Confocal microscopy

The experiment was performed using a LEICA confocal microscope system. The cells were thermostatically controlled and regulated in CO_2. B16F10 cells were grown in 4-well LabTek chambers I at a density of 10,000 cells/well. For localization studies, cells were incubated with 0.6 mg/L with AGuIX® functionalized with FITC as a fluorescent marker for 1 hour. After incubation, cells were rinsed and then incubated with 5 µg/ml fluorescent Alexa Fluor 594 wheat germ agglutinin (Image-iT LIVE Plasma Membrane and Nuclear labeling kit, Life Technologies) for highly selective staining of the plasma membrane for 10 minutes at 37°C and 5 % CO_2. Afterwards, cells were suspended in Hank's balanced salt solution (HBSS) for imaging. FITC was excited at 499 nm, and the fluorescence emission was detected at 520 nm. Alexa Fluor 594 was excited at 592 nm, and emission was detected at 620 nm.

Clonogenic survival assay

Cells were seeded at a density of 40,000 cells/cm^2 and allowed to grow for 18 hours. The cells were incubated 1 hour with 0.6 mg/L with AGuIX® and then irradiated at different doses with 220 kV X-ray at a dose rate of 2 Gy/min. After irradiation, the cells were incubated for 1 hour. Afterwards, the cells were washed, trypsinized, and counted. The cells were then replated in 25-cm^2 flasks and allowed to grow for six divisions (7 days) before staining with a 1 % crystal violet and 10 % ethanol solution. The plates were allowed to dry overnight before being digitally counted for colonies. Clonogenic survival was fitted according to a linear quadratic model of the form SF= $e^{-(\alpha D+\beta D^2)}$, where SF is the surviving fraction, and α and β represent the probabilities of lethal and sub-lethal damage, respectively.[25, 26] The data were normalized to the platting efficiency (PE) of the control condition (0 Gy), *i.e.* PE = number of colony formed after six divisions / number of cells seeded. The experiments were performed in triplicate.

γ-H2AX immunofluorescence assay

After radiation exposure, cells were fixed at two time points, 0.5 and 24 hours, to study the γ-H2AX induction.[27] Cells were fixed with 4 % paraformaldehyde for 20 minutes. After fixation, cells were permeabilized with 0.5 % Triton X-100 and then blocked with 0.2 % skim milk, 0.1 % Triton X-100, and 5 % FBS. The cells were then labeled with the primary antibody anti-phospho-histone H2AX (Merck Millipore) and anti-mouse AlexaFluor-488 secondary antibody (Molecular probes). Coverslips were mounted with VECTASHIELD® mounting medium containing DAPI. γ-H2AX assays were scored using an Axio Imager Z1 fluorescence microscope (Carl Zeiss S.A.S., Le Pecq, France), and the average number of foci was calculated for a minimum of 100 cells per slide. Experimental data represent the average of three independent experiments.

Tumor implantation

The B16F10 cells (50,000 cells) were implanted in the brains of six-week-old C57BL/6J (Janvier, France) as previously described by Lamoral-Theys *et al*.[28] or subcutaneously (10^6 cells suspended in 100 µl culture medium) for the intravital two-photon study. All mice

were housed in a specific pathogen-free (SPF) environment, and procedures were performed in accordance with the Institutional Animal Care and User Committee at the University of Lyon and Grenoble, France. The research involving animals was authorized and was provided an agreement number (L. Sancey, Ph.D., permit number 380922). All efforts were made to minimize the number of animals used and their suffering due to the experimental procedure.

Irradiation set up

For the *in vitro* experiments, radiation exposure was performed using a 220 kV X-ray generator (2 mm Al filter - Precision X-ray Inc., North Branford, CT) at doses ranging from 0 to 8 Gy. Cells were irradiated using a source-to-surface distance of 50 cm and a dose rate of 2 Gy/min. During the *in vivo* experiments, the radiation exposure was performed using a source-to-surface distance of 35 cm, using 320 kV X-ray generator (1.5 mm Al, 0.25 mm Cu, 0.75 mm Sn filter). The dose rate was verified by ionization chamber. The animals were injected intravenously with nanoparticles 3.5 hours before radiation exposure.

Magnetic resonance imaging

Mice were imaged before and after IV injection with 10 mg of AGuIX®. MRI was performed using a 4.7 T scanner (Biospec 47/40 USR AV III, Bruker, Germany; IRMaGe Facility Grenoble) equipped with a 12 cm inner diameter, actively shielded gradient insert (640 mT/m in 120 µs). Actively decoupled volume and surface coils were used for excitation and reception, respectively (Bruker, Germany). Animals were placed in the prone position. All images were acquired in the coronal orientation. The data were processed using Matlab (v7.6, The MathWorks Inc., Natick, MA, USA). The Contrast-to-Noise Ratio (CNR) was computed as the difference between the signal in the tumor and in the healthy tissue, normalized by the SD of the image noise.

Intravital microscopy - two-photon microscopy

Two-photon microscopy was performed as previously described in Sancey *et al*. [29] using an LSM 7MP (Zeiss, Germany) equipped with a 20X water-immersion objective (NA 1.0, Zeiss Jena Germany) and ZEN 2010 software on mice-bearing subcutaneous B16F10 tumors. Laser excitation was performed at 800 nm with a Ti:sapphire laser (Chameleon vision II; Coherent, UK) using a constant laser power of approximately 60 mW. Fluorescence emission was detected by photomultiplier tubes in nondescanned mode with a 492/SP25 nm filter for fluorescence emission, and a 617/73 nm filter (filters from Semrock, US) for red fluorescence emission (rhodamine B).

Small animal radiation

Animals were anesthetized with 2 % isoflurane for the duration of the treatment. Animals treated with AGuIX® (10 mg, IV injection) were exposed to radiation 3.5 hours after injection. Only the head of the animals was placed under the collimated 320 kV beam (12 mm-size). The dose was delivered in 1 fraction of 7 Gy at a dose rate of 2 Gy/min. Prior to the irradiation, the treatment planning system Muriplan (V.1.3.0) was used to calculate the dose distribution in the tumor and in some healthy organs. The radiosensitivity response of the tumor was evaluated using 3 groups composed of 8 to 10 mice each. Animals without nanoparticles and radiation and animals treated with AGuIX® only were merged into a single group of 10 mice because the survival was exactly the same, as previously described in other reports.[30]

Statistical analysis

All experiments were carried out in triplicate with the results expressed as the mean ± standard error (SE). Statistically significant differences were calculated using a two-tailed unpaired t-test or one-way analysis of variance; *p-value*s of < 0.05(*), and < 0.01(**) were considered significant. For *in vivo* investigations, to study the effect of treatment on the survival of B16F10-bearing mice, the mean survival time (MST), standard error (SE), and median survival time (MeST) were calculated for each group using the Kaplan-Meier estimate (Madsen 1986, Statistical concepts prentice Hall, Englewood Cliffs, NJ). A log-rank test was used to determine the p-value for the Kaplan-Meier curve. The p-value for the chi-squared test was calculated using StatsDirect statistics software (StatsDirect Ltd., UK).

Results

Nanoparticle characteristics

The synthesis and main characteristics of AGuIX® have been previously reported.[31, 32] Briefly, AGuIX® are composed of a polysiloxane network surrounded by Gd chelates similar to DOTA (1,4,7,10-tetra-azacyclododecane-1-glutaric anhydride-4,7,10-triacetic acid) that are covalently grafted to an inorganic matrix. The hydrodynamic diameter of the AGuIX® is 3 ± 0.1 nm for a mass of 8.5 ± 1 kDa and a slightly positive zeta potential at pH 7.2, as shown in Figure 1. For some of the experiments, the AGuIX® have been labeled with fluorescein isothiocyanate (FITC).

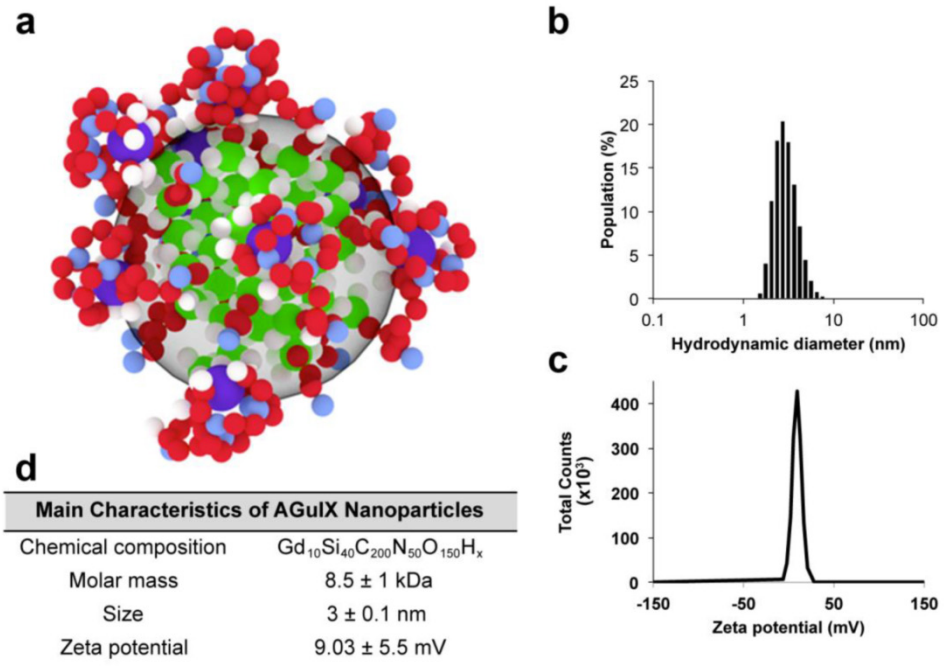

Main Characteristics of AGuIX Nanoparticles	
Chemical composition	$Gd_{10}Si_{40}C_{200}N_{50}O_{150}H_x$
Molar mass	8.5 ± 1 kDa
Size	3 ± 0.1 nm
Zeta potential	9.03 ± 5.5 mV

Figure 1. AGuIX® and their characteristics. (a) Representation of the nanoparticles with the following color code: green = Si, red = C, violet = Gd, blue = N, and white = H; (b) Hydrodynamic diameter of the nanoparticles; (c) Zeta potential of the nanoparticles; (d) Summary of the main characteristics.

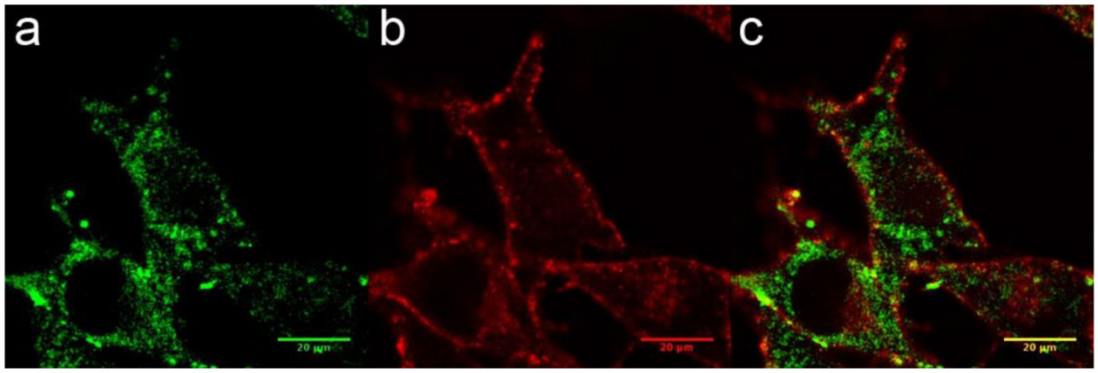

Figure 2. Cellular uptake of AGuIX® in B16F10 cells. (a-c) Fluorescence image of B16F10 cells obtained by confocal microscopy 1 hour after the addition of 0.6 g/L AGuIX® conjugated to FITC (a). The plasma membranes were labeled in red (b), and the merged image is presented in (c).

In vitro investigations

Cell uptake

The internalization of AGuIX® was first investigated. Their cell uptake was observed after 1 hour of incubation with 0.6 mg/L in the cell culture medium, corresponding to 0.4 pg of Gd per cell. This concentration was not toxic to the cells in the absence of radiation exposure and was similar to the values from other *in vitro* investigations using the AGuIX®.[20, 30, 33] Confocal imaging demonstrated that the FITC-labeled particles were located in the cytoplasm of the melanoma cells and inside vesicles (Fig. 2a-c), and confirmed by TEM imaging (Supplementary information). Similarly to previously reported studies on various cell types, B16F10 cells are able to efficiently internalize AGuIX®.[30, 33, 34]

Cell radiation exposure

To assess the efficacy of AGuIX® as radiosensitizers, a clonogenic cell survival assay was performed. As indicated in Figure 3a, compared with control cells, cells incubated with AGuIX® were sensitized to radiation with a sensitivity enhancement ratio (SER) of 2.08 at 2 Gy (Table 1). A dose enhancement fraction (DEF) of 1.3 was calculated from the clonogenic assay results when the AGuIX® were incubated for 1 hour before irradiation. Both the radiation dose inducing 50 % survival (D50%) and the survival fraction at 2 Gy (SF2) decreased in the presence of the nanoparticles. Moreover, the presence of AGuIX® strongly increased the directly lethal damage (increase in α factor), as previously reported for the irradiation of radioresistant head and neck carcinoma cells with these nanoparticles.[30]

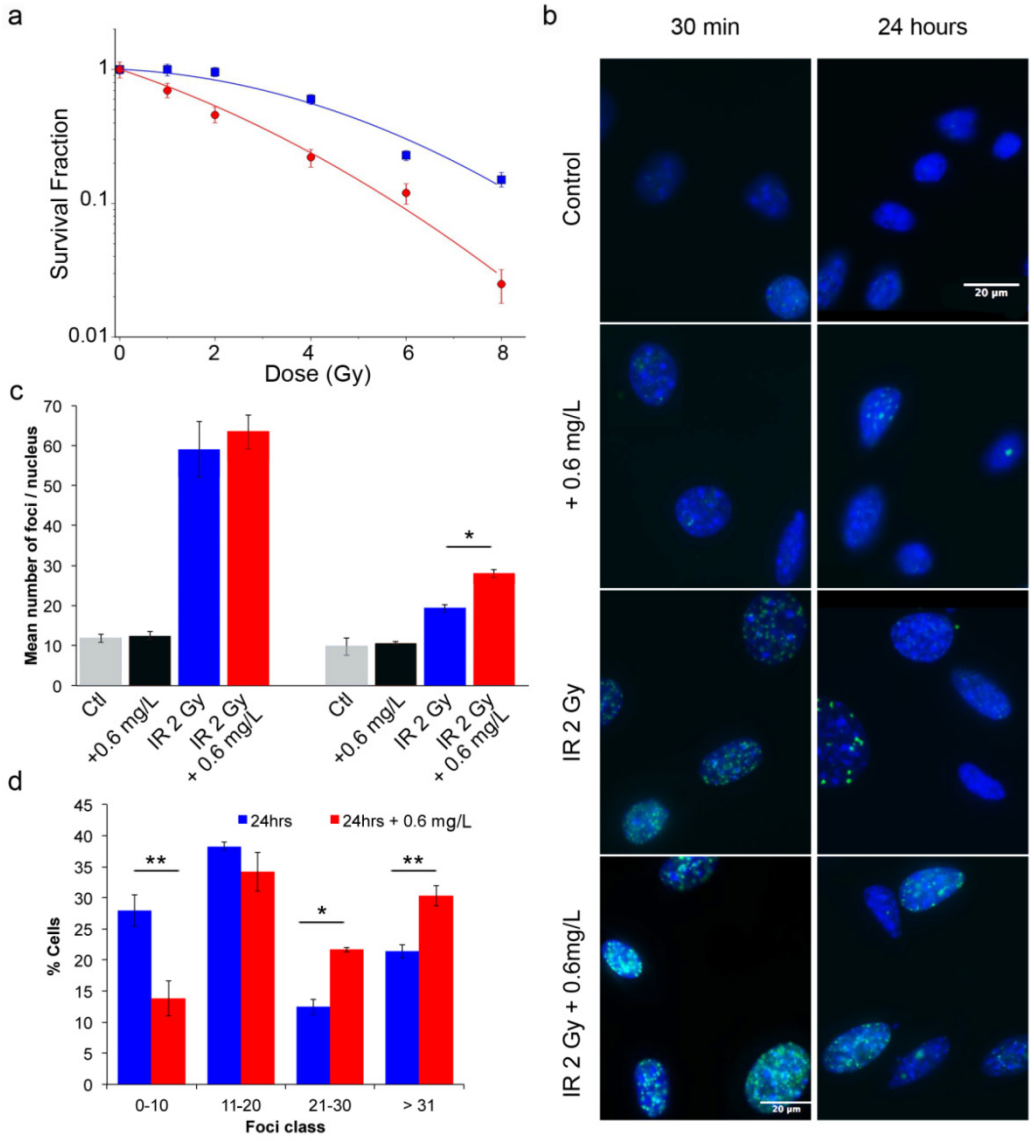

Figure 3. Radiation exposure of B16F10 cells. (a) Surviving fraction of B16F10 after radiation exposure without nanoparticles (blue) and with incubation with 0.6 g/L AGuIX® nanoparticles (red) 1 hour prior to irradiation with 220 kV X-ray. Regression analysis was used to fit the data to a linear quadratic model of the form $\log SF = \alpha * D + \beta * D^2$ (n = 3 / point). (b) Representative images of γ-H2AX foci and (c) their quantification at 0.5 (left panel) and 24 hours (right panel) after exposure to 2 Gy radiation. (d) Percentage of cells having a specific foci class for a total of 350 cells counted per condition. Error bars represent the standard error of the mean of three independent experiments.

Table 1. Radiation response of B16F10 cells untreated or treated with AGuIX®. The sensitivity enhancement ratio (SER) was calculated as the ratio of cell survival without and with AGuIX® treatment at 2 Gy. Additionally, the percentage enhancement factor at 2 Gy was calculated as $\%EF = 100 \times (EF^{2\,Gy}_{Control} - EF^{2\,Gy}_{AGuIX})/EF^{2\,Gy}_{Control}$. DEF is the dose enhancement fraction; SF2 is the survival fraction at 2 Gy.

	α (Gy^{-1})	β (Gy^{-2})	D50% (Gy)	SF2	%EF 2Gy	DEF	SER 2Gy
Control	0.04	0.26	4.5	0.96	-	-	
0.6 mg/L AGuIX	0.26	0.022	1.8	0.46	52 %	1.3	2.08

In addition, γ-H2AX assays provide information on the DNA alteration after cell exposure to radiation through measurement of DNA DSBs. After incubation with the nanoparticles and a 2 Gy radiation exposure, both the initial (0.5 hour) and residual (24 hours) foci were quantified (Fig. 3b-d). The resulting foci were compared to those of the control group (exposed cells without nanoparticle incubation). Thirty minutes after radiation exposure, the induced foci were not significantly different between cells incubated with and without nanoparticles. However, 24 hours after irradiation, the foci disappearance is associated with the DNA damage repair.[35] At this time point, the DNA breaks returned to a low level for the cells that were treated with irradiation alone, reflecting the radioresistance of B16F10 cells. In contrast, DSBs persisted in the cells treated with the combination of radiation and the nanoparticles, resulting in 19.3 ± 0.9 foci/nucleus

versus 28 ± 1 foci/nucleus (p = 0.04), respectively. At 24 hours, the damage observed after irradiation with AGuIX® corresponded to 44 % of the initial damage. Additionally, the combination of radiation exposure and nanoparticles led to a 45 % enhancement in the DSBs compared to the irradiation only. Compared with previous investigations using similar conditions for other tumor cell lines, the response varied at 30 minutes and was slightly lower at 24 hours, indicating a cell type-dependent response.[30] Figure 3d shows that an increasing percentage of cells have a large number of foci (greater than 20 foci) when AGuIX® were used in combination with an external X-ray beam.

In vivo studies

Tumor model and protocol adjustment

To assess the efficacy of AGuIX® as radiosensitizer, a multiple brain metastases model was selected. B16F10 mouse melanoma cells were orthotopically grafted into mouse brains to mimic melanoma brain metastases (Fig. 4a-b), a feature that occurs in a large proportion of melanoma patients and contributes to the exceedingly poor prognosis.[36, 37] As indicated in Figure 4a-b, the cells rapidly formed a main tumor with many metastases that were present in both hemispheres, from the frontal to the occipital lobes.

Imaging was performed on mice to determine the optimal treatment protocol. First, due to the presence of Gd in the nanoparticles, T1-weighted MR imaging was performed at 4.7T 4 and 5 days after tumor implantation. On day 4, the tumors were too small for imaging (not shown), but on day 5, AGuIX® efficiently reached the tumors (Fig 4c). Thus, T1-MRI can efficiently be performed using AGuIX® as contrast agent to visualize the tumor area.

Due to the small size of both the mouse brain and the metastases, most of the time, only the main tumor was observed on day 5, as indicated in Figure 4c, with a CNR of 20.99 for the tumor *vs.* contralateral hemisphere and 59.56 for the tumor *vs.* muscle. Intravital two-photon imaging using fluorescent AGuIX® confirmed the nanoparticle accumulation within the tumor area. In this experiment, the tumor was implanted sub-cutaneously to facilitate the acquisition. A kinetics experiment was performed to determine not only the amount of nanoparticles within the tumor but also their fine distribution within tumor cells and the extracellular matrix (Fig 4d-f). Within the first hour after injection, most of the fluorescence was observed as a diffuse signal in the extracellular environment. Then, from 1 to 3.5 hours, the fluorescence signal increased and assumed the form of small dots within the tumor cells, meaning that some AGuIX® were actively internalized into vesicles over time. The signal was still observed 24 hours after injection with relatively high persistence (31 % compared with that at 1 hour) (Fig 4g).

This study in mice suggests that radiation exposure might be performed from 1 to 24 hours after injection with substantial nanoparticle uptake in tumors and a low background in the surrounding healthy tissue due to both the 21-minute blood half-life [29] of AGuIX® and the absence of extravasation from the normal blood vessels of healthy tissues.

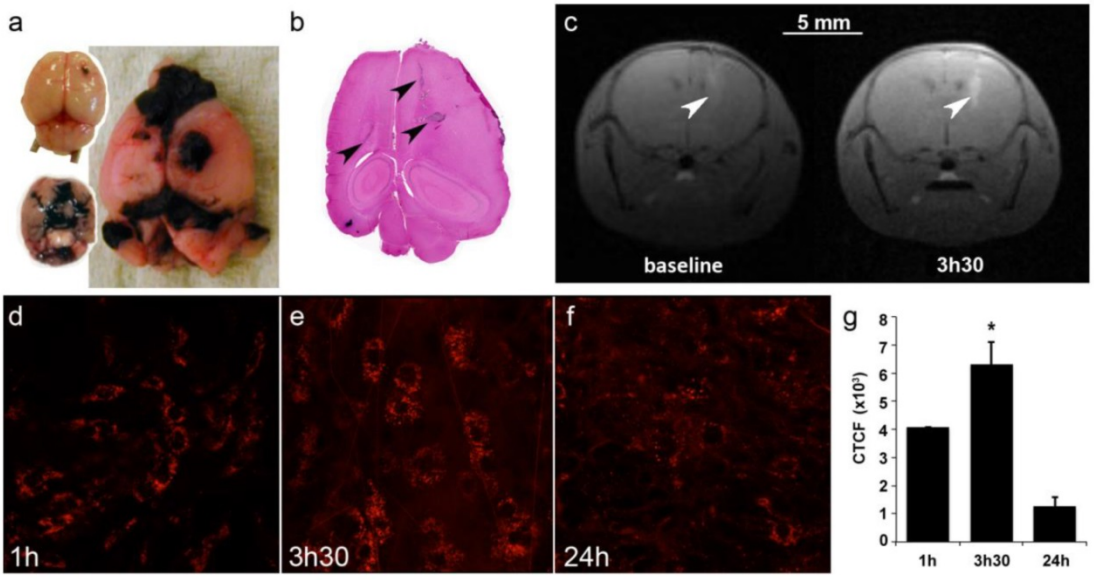

Figure 4. Brain tumor distribution of AGuIX®. (a) Mouse brains 5 and 10 days after B16F10 implantation and (b) the corresponding H&S section. The arrows indicate the localization of tumor metastases. Note that metastases are black due to the high secretion of melanin. (c) T1-weighted images of the brain of B16F10-bearing mouse (spatial resolution of 156 µm). The images were acquired before and 3.5 hours after an intravenous injection of 0.2 ml of particles (50 g/L) at day 5. The tumors were revealed by the T1-positive particles. (d-f) Intravital two-photon microscopy of labeled particles in subcutaneous B16F10 tumors at 1 hour, 3.5 hours and 24 hours after injection, and (g) the corresponding normalized cell fluorescence (CFCT). CFCT was calculated as CFCT = Integrated Density – (Area of selected cell × Mean fluorescence of background reading).

Radiation exposure and overall survival

In common clinical practice, 3D calculations of radiation dose based on imaging and geometrical control of the radiation beams are used to minimize damage to organs-at-risk. In our preclinical study, cone-beam CT was performed prior to the therapy radiation exposure to calculate the expected radiation dose to the brain, the metastases, and other organs at risk, such as eyes. The dose-volume histogram (DVH) showed that 95 % of the brain was covered by the prescription dose (Fig. 5a-b). We also calculated a relative dose of 51.5 % of the prescription for the eyes. While this is higher than typical clinical WBRT procedures, deleterious effects were not observed in our study likely because of the short survival time for all experimental arms

It has been demonstrated that AGuIX® accumulate passively in brain tumors. This phenomenon has previously been reported in brain tumor-bearing animals when the blood brain barrier is damaged.[17, 22, 38] Based on the imaging investigations performed on B16F10 brain metastases (Fig 4c-f), the therapeutic irradiation was performed five days after tumor implantation and at 3.5 hours post IV injection of AGuIX® for highest tumor to healthy tissue ratio. As summarized in Figure 5c and Table 2, the pathology is very aggressive without any animals surviving for more than 14 days after tumor implantation for the control group. After a single 7-Gy radiation exposure, the increase in life span (ILS) was 8.3 % for the animals that were only irradiated and increased to 25 % with the injection of AGuIX® prior to radiation, corresponding to a 3-fold higher treatment efficacy (p=0.0025) when compared with control group. After brain sampling, the metastases were observed in all groups (Fig. 5d).

Table 2. Main survival data. Main survival data of mice bearing B16F10 brain metastases following radiation exposure with or without pre-injection of AGuIX®.

Treatment group	n	Survival time (days)		ILS *vs.* control	
		Mean ± SE	MeST	Mean	MeST
Control	10	11.9 ± 0.6	12	-	-
7 Gy	8	13.7 ± 0.6	13	15.1 %	8.3 %
10 mg + 7 Gy	9	15.4 ± 0.5	15	29.4 %	25 %

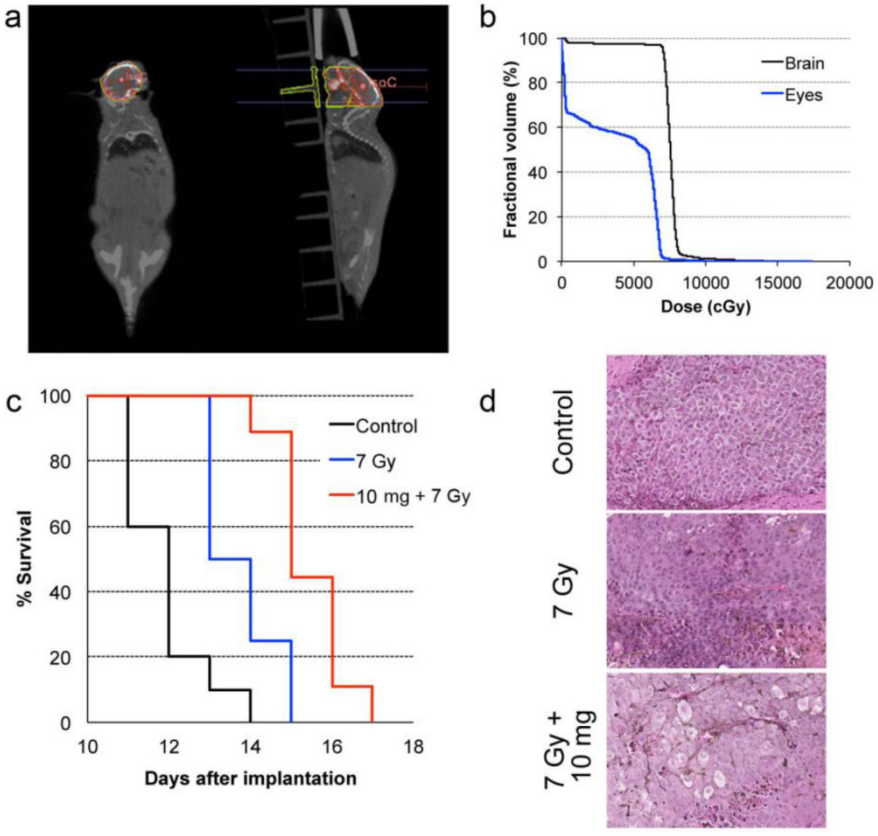

Figure 5. *In vivo* radiation exposure in combination with AGuIX®. (a) Coronal and sagittal views from cone-beam CT performed for the treatment planning. The purple lines correspond to the beam, the red line to the 100 % isodose, the orange line to the 75 % isodose, and the green line to the 5 % isodose. (b) Dose-volume histogram (DVH) showing the percentage of the volume receiving the prescribed dose in the brain region, including the metastases and the eyes (7 Gy in 1 fraction with unique vertical beams). (c) Kaplan-Meier survival curve comparison obtained for brain B16F10 metastases-bearing mice without treatment (black curve, n = 10, including 5 mice injected with particles without radiation exposure), those only treated with 7 Gy radiation exposure (blue curve, n = 8), and those treated with a combination of nanoparticles (10 mg, 3.5 hours after IV injection) and 7 Gy radiation exposure (red curve, n = 9) (p < 0.001). (d) H&E staining of brains in the different conditions. Production of melanin might be observed in the metastases.

Discussion

Improvement of radiation therapy while sparing the healthy surrounding tissue requires either advanced technology [39, 40] or a combination of image-guided therapy with radiosensitization compounds.[20, 41] Among the agents that are able to enhance the radiation dose, high-Z nanoparticles such as the Gd-based AGuIX® have excellent potential as radiosensitizers, principally due to the superior cross-section for high atomic number elements during photon irradiation. Since 2004,[11, 42] Gold nanoparticles have been the subject of *in vitro* and *in vivo* radiosensitization studies including recent papers with improved tumor growth control.[43, 44] Nevertheless, there is no clinical trial currently in progress for radiosensitization using Gold-based nanoparticles. The *in vivo* efficacy of IV injected AGuIX® has recently been reported for aggressive pathologies, such as glioma,[17, 20, 45] pancreatic adenocarcinoma,[46] melanoma [20] and in this paper for brain melanoma metastases. Moreover, due to the presence of Gd, the particles can be used as a T1-positive MRI contrast agent and thus perform the double role of radiosensitizer and imaging agent. The accumulation of AGuIX® in the tumor occurs through the enhanced permeability and retention (EPR) effect.[16, 17, 20] Efficient renal elimination of AGuIX® has been demonstrated elsewhere.[29] The tumor to healthy tissues ratio of IV injected AGuIX® is highly favorable for both imaging and therapy for a window of several hours, although the exact kinetics will be patient and tumor specific.[17, 20]

In this study, we demonstrated that the AGuIX® are internalized *in vitro* in small vesicles in the B16F10 cells. This internalization has been observed using both fluorescent and label-free nanoparticles. *In vitro*, a dose enhancement fraction (DEF) of 1.3 was calculated from the clonogenic assay. This radiosensitization is correlated to the enhancement of DNA DSBs, and to the augmentation of the number of cells presenting a high number of foci (Fig. 3d). These results are in concordance with previous *in vitro* studies.[30, 33, 34] The AGuIX® reached the tumor after IV administration and were internalized into cells in small vesicles, similar to *in vitro* accumulation, from 1 hour to 24 hours in this model. The radiosensitization was also demonstrated *in vivo* with an increase of the animal's lifespan after treatment by the combination of AGuIX® and radiotherapy.

Clinically, AGuIX® could be useful for several clinical applications. In addition to enhanced radiation therapy, MRI contrast enhancement would be beneficial for treatment planning simulation, patient set-up and real-time guidance. Tumor delineation should be much improved over CT-only imaging. If confirmed in humans, the long-term persistence of AGuIX® in tumor cells may enable dose enhancement for multiple radiation treatments. Extensive studies performed in rodents and non-human primates, demonstrated no adverse effects even at high repeated doses (to be published separately). These studies combined supply a strong rationale for a future clinical trial with AGuIX®.

Conclusion

In summary, we have demonstrated the therapeutic efficacy of Gd-based nanoparticles, AGuIX®, as a radiosensitizer in an aggressive pathology, *i.e.* multiple brain metastases. In addition, AGuIX® are effective T1-MRI contrast agents. The combination of AGuIX® and irradiation created significant dose enhancement *in vitro*, and improved the survival of mice bearing aggressive brain tumors. This study demonstrated the safety and efficacy of AGuIX® as a potential clinical contrast agent and radiosensitizer.

Supplementary Material

Figures S1. http://www.thno.org/v06p0418s1.pdf

Abbreviations

AGuIX®: activation-guided irradiation by X-ray; WBRT: whole-brain radiotherapy; ROS: reactive oxygen species; EPR: enhanced permeability and retention; MRI: magnetic resonance imaging; EF: enhancement factor; DSB: double strand breaks; DOTA: 1,4,7,10-tetra-azacyclodecane-1-gutaric anhydride-4,7,10-triacetic acid; H&E: hematoxylin and eosin; FITC: fluorescein isothiocyanate; TEM: transmission electron microscopy; DEF: dose enhancement fraction; SF: survival fraction; SER: sensitivity enhancement ratio; CNR: contrast to noise ratio; CT: computed tomography; DHV: dose volume histogram; ILS: increase in life span.

Acknowledgements

The authors gratefully acknowledge the LABEX PRIMES (ANR-11-LABX-0063) of Lyon 1 University within the program "Investissements d'Avenir" (ANR-11-IDEX-0063), which was operated by the French National Research Agency (ANR) within the ANR Multimage ANR-12-RPIB-0010, as well as the Lyon Science Transfert, for financial support. TPLSM imaging was performed at the Two-Photon Microscopy Platform (GIS-IBiSA ISdV), Photonic Imaging Center, Grenoble Institute of Neuroscience. The MRI facility IRMaGe is partly funded by the French program 'Investissement d'Avenir' run by the French National Research Agency, grant 'Infrastructure d'avenir en Biologie Santé' - ANR-11-INBS-0006. We

also wholeheartedly acknowledge the CTμ of Villeurbanne (A. Rivoire and C. Boule), the animal facility of Lyon Sud (P. Manas) and of Optimal – Grenoble (J. Vollaire and V. Josserand), C. Cadet and the EMR3837 team for fruitful discussions and technical help, and F. Rossetti and M. Bonnel for AGuIX® synthesis.

Author contributions

L.S., S.K., and O.T. designed and conceived the experiments. S.K., A.D., F.A., H.G., E.B., and L.S. performed the experiments and/or analyzed the data. F.L. helped with the *in vivo* model of multiple brain metastases. F. Lux and P.M. produced the particles, particularly the fluorescent particles. C.R-L., R.B., C.V. and O.T. provided technical support and conceptual advice. L.S. and S.K. wrote the manuscript. All authors contributed to the final manuscript.

Competing Interests

F Lux, and O Tillement have one patent to disclose: WO2011135101. This patent protects some of the nanoparticles described in this publication: AGuIX®. The authors have no other relevant affiliations or financial involvement with any organization or entity with a financial interest in or financial conflict with the subject matter or materials discussed in the manuscript apart from those disclosed.

References

1. Fonkem E, Uhlmann EJ, Floyd SR, Mahadevan A, Kasper E, Eton O, et al. Melanoma brain metastasis: overview of current management and emerging targeted therapies. Expert review of neurotherapeutics. 2012; 12: 1207-15.
2. Hodi FS, O'Day SJ, McDermott DF, Weber RW, Sosman JA, Haanen JB, et al. Improved survival with ipilimumab in patients with metastatic melanoma. The New England journal of medicine. 2010; 363: 711-23.
3. Robert C, Long GV, Brady B, Dutriaux C, Maio M, Mortier L, et al. Nivolumab in previously untreated melanoma without BRAF mutation. The New England journal of medicine. 2015; 372: 320-30.
4. Li J, Wang Y, Liang R, An X, Wang K, Shen G, et al. Recent advances in targeted nanoparticles drug delivery to melanoma. Nanomedicine. 2015; 11: 769-94.
5. Sampson JH, Carter JH, Jr., Friedman AH, Seigler HF. Demographics, prognosis, and therapy in 702 patients with brain metastases from malignant melanoma. Journal of neurosurgery. 1998; 88: 11-20.
6. Patchell RA, Tibbs PA, Regine WF, Dempsey RJ, Mohiuddin M, Kryscio RJ, et al. Postoperative radiotherapy in the treatment of single metastases to the brain: a randomized trial. JAMA Dermatology. 1998; 280: 1485-9.
7. Patel KR, Burri SH, Asher AL, Crocker IR, Fraser RW, Zhang C, et al. Comparing Preoperative With Postoperative Stereotactic Radiosurgery for Resectable Brain Metastases: A Multi-institutional Analysis. Neurosurgery. 2015.
8. Scoccianti S, Ricardi U. Treatment of brain metastases: review of phase III randomized controlled trials. Radiotherapy and Oncology. 2012; 102: 168-79.
9. Yaeh A, Nanda T, Jani A, Rozenblat T, Qureshi Y, Saad S, et al. Control of brain metastases from radioresistant tumors treated by stereotactic radiosurgery. Journal of Neurooncology. 2015; 124: 507-14.
10. Mehta MP, Rodrigus P, Terhaard CH, Rao A, Suh J, Roa W, et al. Survival and neurologic outcomes in a randomized trial of motexafin gadolinium and whole-brain radiation therapy in brain metastases. Journal of Clinical Oncology. 2003; 21: 2529-36.
11. Hainfeld JF, Slatkin DN, Smilowitz HM. The use of gold nanoparticles to enhance radiotherapy in mice. Physics in medicine and biology. 2004; 49: N309-15.
12. Berbeco RI, Ngwa W, Makrigiorgos GM. Localized dose enhancement to tumor blood vessel endothelial cells via megavoltage X-rays and targeted gold nanoparticles: new potential for external beam radiotherapy. International journal of radiation oncology, biology, physics. 2011; 81: 270-6.
13. Lux F, Sancey L, Bianchi A, Cremillieux Y, Roux S, Tillement O. Gadolinium-based nanoparticles for theranostic MRI-radiosensitization. Nanomedicine. 2015; 10: 1801-15.
14. Retif P, Pinel S, Toussaint M, Frochot C, Chouikrat R, Bastogne T, et al. Nanoparticles for Radiation Therapy Enhancement: the Key Parameters. Theranostics. 2015; 5: 1030-44.
15. Sicard-Roselli C, Brun E, Gilles M, Baldacchino G, Kelsey C, McQuaid H, et al. A new mechanism for hydroxyl radical production in irradiated nanoparticle solutions. Small. 2014; 10: 3338-46.
16. Dufort S, Sancey L, Coll JL. Physico-chemical parameters that govern nanoparticles fate also dictate rules for their molecular evolution. Advanced Drug Delivery Reviews. 2012; 64: 179-89.
17. Le Duc G, Miladi I, Alric C, Mowat P, Brauer-Krisch E, Bouchet A, et al. Toward an image-guided microbeam radiation therapy using gadolinium-based nanoparticles. ACS Nano. 2011; 5: 9566-74.
18. Luchette M, Korideck H, Makrigiorgos M, Tillement O, Berbeco R. Radiation dose enhancement of gadolinium-based AGuIX nanoparticles on HeLa cells. Nanomedicine. 2014; 10: 1751-5.
19. Porcel E, Tillement O, Lux F, Mowat P, Usami N, Kobayashi K, et al. Gadolinium-based nanoparticles to improve the hadrontherapy performances. Nanomedicine. 2014; 10: 1601-8.
20. Sancey L, Lux F, Kotb S, Roux S, Dufort S, Bianchi A, et al. The use of theranostic gadolinium-based nanoprobes to improve radiotherapy efficacy. The British Journal of Radiology. 2014; 87: 20140134.
21. Bianchi A, Lux F, Tillement O, Cremillieux Y. Contrast enhanced lung MRI in mice using ultra-short echo time radial imaging and intratracheally administrated Gd-DOTA-based nanoparticles. Magnetic Resonance in Medicine. 2013; 70: 1419-26.
22. Bianchi A, Moncelet D, Lux F, Plissonneau M, Rizzitelli S, Ribot EJ, et al. Orotracheal administration of contrast agents: a new protocol for brain tumor targeting. NMR in Biomedicine. 2015; 28: 738-46.
23. Detappe A, Rottmann J, Kunjachan S, Tillement O, Berbeco R. MO-FG-BRA-07: Theranostic Gadolinium-Based AGuIX Nanoparticles for MRI-Guided Radiation Therapy. Medical Physics. 2015; 42: 3566.
24. Nascimento FD, Sancey L, Pereira A, Rome C, Oliveira V, Oliveira EB, et al. The natural cell-penetrating peptide crotamine targets tumor tissue in vivo and triggers a lethal calcium-dependent pathway in cultured cells. Molecular Pharmaceutics. 2012; 9: 211-21.
25. Franken NA, Rodermond HM, Stap J, Haveman J, van Bree C. Clonogenic assay of cells in vitro. Nature Protocols. 2006; 1: 2315-9.
26. Barendsen GW. Parameters of linear-quadratic radiation dose-effect relationships: dependence on LET and mechanisms of reproductive cell death. International Journal of Radiation Biology. 1997; 71: 649-55.
27. Mariotti LG, Pirovano G, Savage KI, Ghita M, Ottolenghi A, Prise KM, et al. Use of the gamma-H2AX assay to investigate DNA repair dynamics following multiple radiation exposures. PLoS One. 2013; 8: e79541.
28. Lamoral-Theys D, Andolfi A, Van Goietsenoven G, Cimmino A, Le Calve B, Wauthoz N, et al. Lycorine, the main phenanthridine Amaryllidaceae alkaloid, exhibits significant antitumor activity in cancer cells that display resistance to proapoptotic stimuli: an investigation of structure-activity relationship and mechanistic insight. Journal of Medicinal Chemistry. 2009; 52: 6244-56.
29. Sancey L, Kotb S, Truillet C, Appaix F, Marais A, Thomas E, et al. Long-term in vivo clearance of gadolinium-based AGuIX nanoparticles and their biocompatibility after systemic injection. ACS Nano. 2015; 9: 2477-88.
30. Miladi I, Aloy MT, Armandy E, Mowat P, Kryza D, Magne N, et al. Combining ultrasmall gadolinium-based nanoparticles with photon irradiation overcomes radioresistance of head and neck squamous cell carcinoma. Nanomedicine. 2015; 11: 247-57.
31. Lux F, Mignot A, Mowat P, Louis C, Dufort S, Bernhard C, et al. Ultrasmall rigid particles as multimodal probes for medical applications. Angewandte Chemie International Edition. 2011; 50: 12299-303.
32. Mignot A, Truillet C, Lux F, Sancey L, Louis C, Denat F, et al. A top-down synthesis route to ultrasmall multifunctional Gd-based silica nanoparticles for theranostic applications. Chemistry. 2013; 19: 6122-36.
33. Rima W, Sancey L, Aloy MT, Armandy E, Alcantara GB, Epicier T, et al. Internalization pathways into cancer cells of gadolinium-based radiosensitizing nanoparticles. Biomaterials. 2013; 34: 181-95.
34. Stefancikova L, Porcel E, Eustache P, Li S, Salado D, Marco S, et al. Cell localisation of gadolinium-based nanoparticles and related radiosensitising efficacy in glioblastoma cells. Cancer Nanotechnology. 2014; 5: 6.
35. Rogakou EP, Pilch DR, Orr AH, Ivanova VS, Bonner WM. DNA double-stranded breaks induce histone H2AX phosphorylation on serine 139. The Journal of Biological Chemistry. 1998; 273: 5858-68.
36. Taillibert S, Le Rhun E. [Epidemiology of brain metastases]. Cancer radiotherapie : journal de la Societe francaise de radiotherapie oncologique. 2015; 19: 3-9.
37. Vecchio S, Spagnolo F, Merlo DF, Signori A, Acquati M, Pronzato P, et al. The treatment of melanoma brain metastases before the advent of targeted therapies: associations between therapeutic choice, clinical symptoms and outcome with survival. Melanoma Research. 2014; 24: 61-7.
38. Bechet D, Auger F, Couleaud P, Marty E, Ravasi L, Durieux N, et al. Multifunctional ultrasmall nanoplatforms for vascular-targeted interstitial photodynamic therapy of brain tumors guided by real-time MRI. Nanomedicine. 2015; 11: 657-70.

39. Frakes JM, Figura ND, Ahmed KA, Juan TH, Patel N, Latifi K, et al. Potential role for LINAC-based stereotactic radiosurgery for the treatment of 5 or more radioresistant melanoma brain metastases. Journal of Neurosurgery. 2015: 1-7.
40. De Felice F, Musio D, Cassese R, Tombolini V. Radiotherapeutic treatment approaches for brain metastases. Anticancer Research. 2014; 34: 6913-8.
41. Moding EJ, Kastan MB, Kirsch DG. Strategies for optimizing the response of cancer and normal tissues to radiation. Nature Reviews Drug Discovery. 2013; 12: 526-42.
42. Hainfeld JF, Dilmanian FA, Zhong Z, Slatkin DN, Kalef-Ezra JA, Smilowitz HM. Gold nanoparticles enhance the radiation therapy of a murine squamous cell carcinoma. Physics in Medicine and Biology. 2010; 55: 3045-59.
43. Joh DY, Kao GD, Murty S, Stangl M, Sun L, Al Zaki A, et al. Theranostic gold nanoparticles modified for durable systemic circulation effectively and safely enhance the radiation therapy of human sarcoma cells and tumors. Translational Oncology. 2013; 6: 722-31.
44. Su N, Dang Y, Liang G, Liu G. Iodine-125-labeled cRGD-gold nanoparticles as tumor-targeted radiosensitizer and imaging agent. Nanoscale Research Letters. 2015; 10: 160.
45. Le Duc G, Roux S, Paruta-Tuarez A, Dufort S, Brauer E, Marais A, et al. Advantages of gadolinium based ultrasmall nanoparticles vs molecular gadolinium chelates for radiotherapy guided by MRI for glioma treatment. Cancer Nanotechnology. 2014; 5.
46. Detappe A, Kunjachan S, Rottmann J, Robar J, Tsiamas P, Korideck H, et al. AGuIX nanoparticles as a promising platform for image-guided radiation therapy. Cancer Nanotechnology. 2015;6: 4.